Journal of Electroanalytical Chemistry 929 (2023) 117114

Contents lists available at ScienceDirect

Journal of Electroanalytical Chemistry

journal homepage: www.elsevier.com/locate/jelechem

Stability of a pyrimidine-based dye-sensitized TiO_2 photoanode in sacrificial electrolytes

A. Ansón-Casaos [a,*], C. Martínez-Barón [a], S. Angoy-Benabarre [a], J. Hernández-Ferrer [a], A.M. Benito [a], W.K. Maser [a], M.J. Blesa [b]

[a] Instituto de Carboquimica, ICB-CSIC, Zaragoza, Spain
[b] Department of Organic Chemistry, INMA, University of Zaragoza-CSIC, Zaragoza, Spain

ARTICLE INFO

Keywords:
Water splitting
Photoelectrochemistry
Semiconductor oxides
Dye-sensitizer
Pyrimidine

ABSTRACT

Dye sensitization of semiconductor metal oxides aims to extend the light absorption range into the visible region, of particular interest for their use as photoanodes in photoelectrochemical (PEC) water splitting. Organic dyes, however, suffer from limited chemical stability when they are exposed to constant potential and irradiation in aqueous media. Thus, in this work, we evaluate a novel metal-free donor-π-acceptor (D-π-A) dye (AT-Pyri), demonstrating significant sensitization of film photoanodes based on TiO_2 nanoparticles. Among a series of tested sacrificial agents, the addition of triethanolamine (TEOA) to the sodium sulphate electrolyte prevents the degradation of AT-Pyri even after several hours of operation. Combining two sacrificial agents (methanol and TEOA) results in a synergetic improvement of the PEC water-splitting activity. Notably, the stabilization of the AT-Pyri photoanode is accompanied by a substantial increase in the photocurrent over the reference TiO_2 photoanode, while the associated spikes in transient photocurrent measurements disappear.

1. Introduction

Sensitization of TiO_2 with organic products has been largely studied as a method to improve its solar photocatalytic activity toward water splitting [1]. Organic sensitizers include ruthenium-based compounds, various types of metal complexes, carbon dots, and metal-free organic dyes [2–4]. Organic dye sensitization has been studied in photoanodes [5,6], photocathodes [7], and tandem cells [8]. One of the most typical drawbacks of organic dyes is their low stability under continuous photoelectrochemical (PEC) operation and irradiation conditions.

Donor-π-acceptor (D-π-A) dyes are versatile metal-free organic compounds in which intramolecular charge transfer (ICT) between donor and acceptor moieties takes place [9]. The adequate choice of structural units (D, π, A) facilitates the optimization of the molecular energy levels, providing a broad intense light absorption for photochemical applications. Regarding donors, molecules such as coumarin, phenothiazine, carbazole, triphenylamine (TPA) and indole have been tested [9]. Also, *N,N'*-dialkylanilines offer suitable light absorption and sensitization properties when used in dye-sensitized photovoltaic cells, showing a red-shifted ICT band with respect to TPA derivatives [10,11]. Regarding π-spacers, thiophenes have been proven to stabilize the oxidized form of certain dyes in water [12]. Finally, the most commonly used acceptor moiety is the cyanoacetic group due to the strong electron-withdrawing ability of the cyano group, and its easy linkage to TiO_2 through the carboxylic group [13]. However, the hydrolyzation of the ester bond between the carboxylic anchoring group and TiO_2, in an aqueous environment or under alkaline conditions, leads to the desorption of dye molecules, limiting the activity of the sensitized photoanode. As an alternative, dyes bearing pyridine groups have shown improved adsorption on TiO_2 compared to phosphonate and carboxylate groups [14]. Similarly, pyrimidine has electron withdrawing properties and can act as an acceptor group in D-π-A dyes. Nitrogen atoms from the pyrimidine also allow chelation, protonation and hydrogen-bond formation. Therefore, we designed a D-π-A system with *N,N'*-dialkylaniline as a donor, thiophene as a π-spacer and pyrimidine as both, an anchoring and an acceptor group for PEC water splitting.

Transient photocurrent measurements in D-π-A dye/TiO_2 electrodes reveal photocurrent spikes and decays, which have been associated with charge trapping processes [15]. Specifically, it has been suggested that the D-π-A dye evolves into an oxidized state [D-π-

* Corresponding author.
E-mail address: alanson@icb.csic.es (A. Ansón-Casaos).

https://doi.org/10.1016/j.jelechem.2022.117114
Received 31 October 2022; Received in revised form 20 December 2022; Accepted 22 December 2022
Available online 24 December 2022

A]$^+$, and might undergo chemical changes, most probably decomposition, depending on the stability of the [D-π-A]$^+$ state [15]. Improvements in the charge transfer, which will likely lead to a decrease in adverse effects of accumulation, can be achieved by incorporating water oxidation catalysts on the electrode [16–18]. The response and stability of D-π-A dyes have been also improved by the insertion of an auxiliary acceptor group in the molecule [19]. Despite these considerations, PEC experiments on D-π-A dye-sensitized electrodes are typically performed in the presence of sacrificial agents: hydroquinone [15], ascorbic acid [20], Na_2S/Na_2SO_3 [21], triethanolamine (TEOA) [22,23], etc.

Sacrificial agents, which have been added for years to improve photocatalytic performance, are recurrent and can be well classified into a few categories [24]. Methanol (MeOH) and amines rise the photocurrent in most types of photoelectrodes [25,26]. Iodide has been extensively used in dye-sensitized photovoltaic cells and tried for photocatalytic hydrogen production [27,28]. In particular, TEOA has been often added to complex photocatalytic systems for hydrogen evolution [29–32]. However, direct comparisons of the activity of those common sacrificial agents are scarce [33].

In this work, we thus focus on the effect of adding sacrificial agents (MeOH, glycerin, diethylenediamine, EDTA, hydroquinone, KI, TEOA) on the activity and stability of both, a reference TiO_2 photoanode, and another TiO_2 electrode that is sensitized by the AT-Pyri D-π-A dye. The pH of the electrolyte is kept nearly neutral, avoiding strong acid and alkaline environments. In addition, we consider the behaviour after adding mixtures of MeOH and TEOA, and we observe a kind of synergetic interaction resulting in an improved PEC water splitting activity. To the best of our knowledge, that synergetic effect has not been reported before. Finally, we specifically observe a relationship between the outcome of typical PEC characterization methods and the stability of the dye in a 5 h experiment.

2. Experimental

2.1. Synthesis of AT-Pyri

The synthesis of the AT-Pyri dye, including the detailed experimental procedure and complete characterization, has been published elsewhere [34]. Briefly, the aldehyde 5-(4-dimethylaminophenyl) thiophenyl-2-carbaldehyde (AT-CHO) was prepared following a literature procedure [35]. The compound AT-Pyri was prepared by condensation between AT-CHO and 4-methylpyrimidine. A phase-transfer catalyst (Aliquat 336) was used at reflux in aqueous NaOH. This method gives the AT-Pyri dye in a yield of 48 % [34]. The detailed experimental method and the molecule characterization are included in the Supporting Information.

2.2. TiO_2 deposition and sensitization

FTO-coated glass substrates (80 Ω/sq., 80 nm, 25 × 10 × 1.1 mm^3) were cleaned by the subsequent immersion in ultra-pure water with Hellmamex III, ultra-pure water, and ethanol for 15 min under sonication. Substrates were calcined at 500 °C in air for 30 min and treated under ozone for 25 min. Once the cleaning process was done, the deposition of the TiO_2 paste (GreatCell Solar, 18 NR-AO) was performed by screen printing. The paste was sintered in an oven by the heating program: 5 min at 325 °C, 5 min at 375 °C, 5 min at 450 °C and 15 min at 500 °C. The covered surface and the amount of paste were 1 cm^2 and 0.6 mg/cm^2, respectively. The width of the TiO_2 layer was approximately 4.5 μm, measured with the profilometer Dektak XT.

For the adsorption of AT-Pyri, TiO_2 film substrates were immersed in a 0.1 mM dichloromethane solution of AT-Pyri for 72 h in the dark. They were subsequently cleaned with dichloromethane and dried with a N_2 stream. The quantity of loaded dye was determined to be $1.72{\cdot}10^{-7}$ mol·cm^{-2}.

2.3. Characterization and photoelectrochemical techniques

UV–vis spectra were recorded with Cary 6000 spectrometer. Scanning electron microscopy (SEM) was performed in an SEM-EDX Hitachi S-3400 N. Attenuated total reflection (ATR) FTIR spectra were recorded in a Perkin-Elmer Spectrum 100 FT-IR spectrometer. Micro Raman spectra were measured in a HORIBA Jobin Yvon Raman spectrometer HR 800UV, using a 532 nm laser.

The photoelectrochemical experiments were performed using an Autolab PGSTAT302 from MetroOhm. The light source was a 150 W xenon lamp in a laboratory solar simulator from LOT-Oriel. The lamp was set at its maximum intensity, thus providing an incident power of approximately 100 mW·cm^{-2} AM1.5G at the distance of the target electrode. The photoelectrochemical cell consisted of a glass container with a quartz window and three electrodes, including the Ag/AgCl electrode as the reference (3 M NaCl, E° = 0.210 V vs SHE) and a graphite bar as the counter electrode. The supporting electrolyte was always an aqueous 0.1 M Na_2SO_4 solution, and it was purged with N_2 for 10 min before the measurement. The cyclic voltammetry (CV) experiments were performed at 20 mV·s^{-1} in the range of −1.4 to 0.4 V, starting at 0.4 V vs Ag/AgCl, both in the dark and under irradiation conditions. The on/off transient photocurrent experiments were performed at a constant voltage of 0 V (vs Ag/AgCl). On each working electrode, we performed all the PEC experiments subsequently and in the following order: CV in the dark, transient photocurrent, and CV under irradiation. The monochromator (LOT Oriel MSH-300) is utilized to study the photocurrent as a function of the incident wavelength, and thus to corroborate the sensitization capability of AT-Pyri within the TiO_2 photoanode.

3. Results and discussion

The AT-Pyri dye molecule consists of aniline as the electron-donating group, thiophene as a π-spacer, and pyrimidine as the electron withdrawing and anchoring group (Fig. 1.a). The optical and electrochemical characteristics of the AT-Pyri molecule are summarized in Fig. 1 and in the Supporting Information. Fig. 1 also shows the spectroscopic and SEM characterization of TiO_2 and AT-Pyri/TiO_2 electrodes. The UV–vis spectrum of the AT-Pyri molecule in CH_2Cl_2 solution (Fig. 1.b) shows a band in the range of 350–500 nm, which is attributed to the ICT between the electron-donating and the electron-withdrawing part of the dye molecule [34]. The spectrum of the AT-Pyri/TiO_2 film exhibits a hypsochromic shift of the ICT band compared to the measurement in solution, which can be associated with the linkage of the dye on the TiO_2 film [35] and to an *H*-aggregation effect. SEM images of TiO_2 (Fig. 1.c) and AT-Pyri/TiO_2 (Fig. 1.d) show that the dye was adsorbed on the granular TiO_2 film, resulting in surface smoothing.

The ATR-FTIR spectrum (Fig. 1.e) of the AT-Pyri dye powder displays several peaks, including the stretching vibration of C=C at ca. 1600 cm^{-1} and C=N at 1573 and 1439 cm^{-1}. For comparison, the ATR-FTIR spectrum of AT-Pyri/TiO_2 was measured on powder material from scratched electrodes. Some of the main vibration bands of the AT-Pyri molecule are upshifted upon the interaction with TiO_2. Specifically, the C=N bands appear at 1602 and 1450 cm^{-1}, indicating the coordination between the nitrogen of pyrimidine rings and the acid Ti^{n+} sites on TiO_2 [36–39]. Raman spectra (Fig. 1.f) show signals at around 140, 400, 520 and 640 cm^{-1}, which are due to modes of TiO_2 anatase phase, E_g, B_{1g}, B_{1g} + A_{1g} and E_g respectively [40]. In the AT-Pyri/TiO_2 spectrum, additional signals are observed in the range of 1000–1600 cm^{-1}, which can be attributed to the AT-Pyri system. In particular, the stretching mode of the thiophene ring at

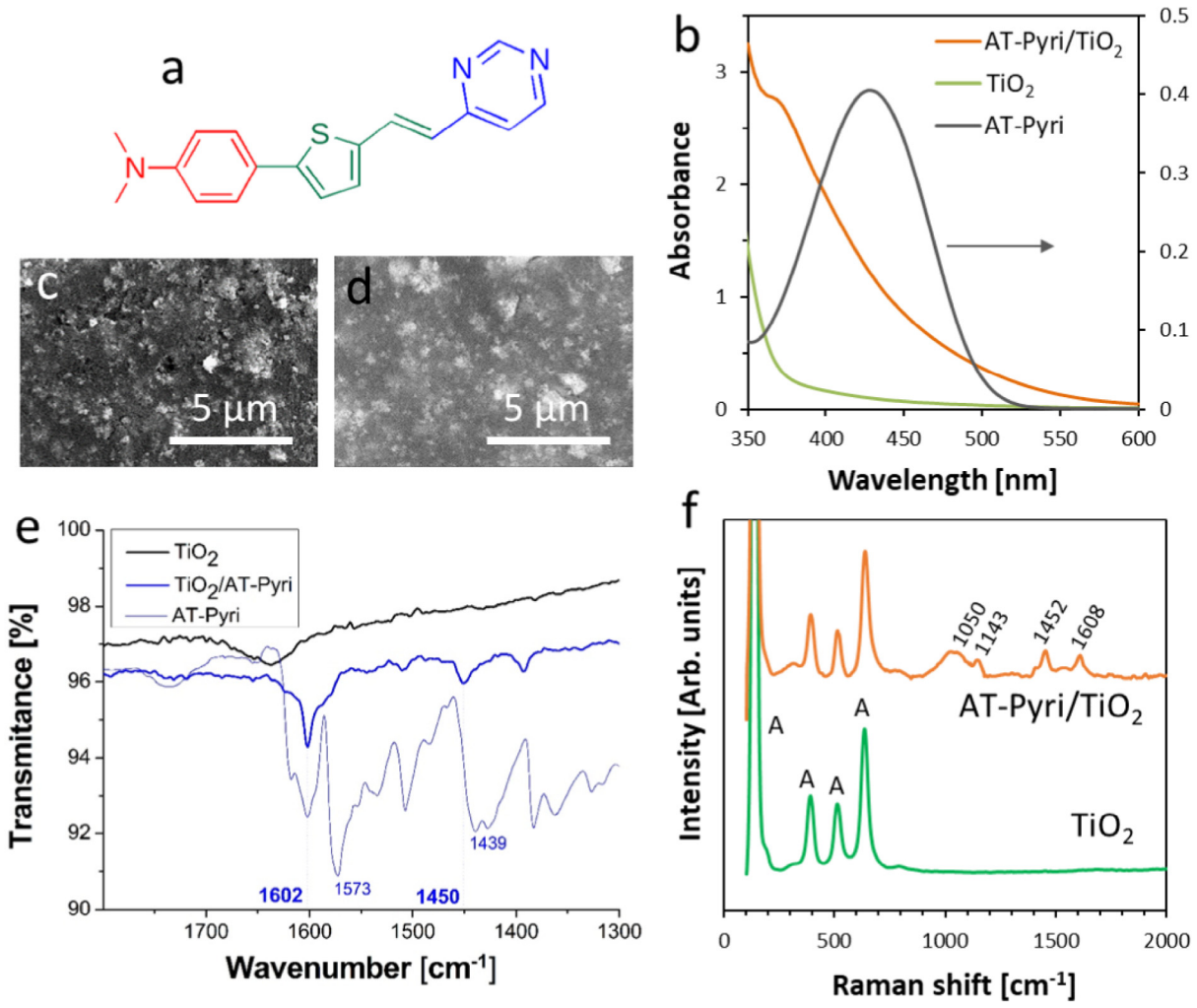

Fig. 1. Characterization of the AT-Pyri dye and AT-Pyri/TiO_2 electrodes: a) Molecular D-π-A structure of the AT-Pyri dye; b) UV–vis absorption spectra of a 0.02 mM AT-Pyri solution in CH_2Cl_2, and the AT-Pyri/TiO_2 electrode prepared by 72 h of immersion in a 0.1 mM solution; c) SEM image of a TiO_2 electrode (top view); d) SEM image of the AT-Pyri/TiO_2 electrode; e) ATR-FTIR spectra; and f) Micro-Raman spectra at 532 nm on TiO_2 and AT-Pyri/TiO_2 electrodes.

1380 cm^{-1} underlines the molecule aromatic character [41]. It is noteworthy that the shoulder at around 1400 cm^{-1} and peaks at 1452 and 1608 cm^{-1} are analogous to the main bands of the ATR-FTIR spectrum.

The photoelectrochemical characterization of the TiO_2 and AT-Pyri/TiO_2 electrodes in aqueous Na_2SO_4 at nearly neutral pH is presented in Fig. 2. In the dark (Fig. 2.a), the CV measurement of bare TiO_2 shows a quite reversible cycle, except for certain features in the 1st cathodic scan, which are related to reduction reactions of the TiO_2 surface, probably with a loss of oxygen. The first CV scan for the AT/Pyri/TiO_2 electrode evidences an irreversible reduction feature due to AT-Pyri at −0.6 and −0.4 V. Tentatively, this signal might be assigned to an interaction between nitrogen of the pyrimidine ring and hydrogen atoms or ions from the electrolyte. For subsequent CV scans in the dark, the AT-Pyri/TiO_2 electrode is quite stable. Only a small reduction feature at ca. −0.35 V, which might be assigned to some electron trapping effect in the AT-Pyri/TiO_2 interface, remains in the 2nd cycle.

Under light irradiation (Fig. 2.b), the CV plot shows the rise of a photocurrent (j_{ph}) at $E > -0.6$ V vs Ag/AgCl. The 1st and 2nd cycles for the bare TiO_2 electrode are nearly identical, so we only represent the 2nd cycle in Fig. 2.b. On the contrary, the AT-Pyri/TiO_2 electrode unveils a photocurrent activation from the 1st to the 2nd cycle. The final j_{ph} value of the AT-Pyri/TiO_2 electrode is notably higher than that of blank TiO_2. In addition, a redox couple at $E = -0.1$ and $E = -0.5$ V can be related to the appearance of the oxidized form AT-Pyri$^+$ [15]. The AT-Pyri$^+$ form is relatively stable under CV cycles, in agreement with previous observations on other chemically related dyes [15].

Transient photocurrent measurements (Fig. 2.c and 2.d) unveils prominent spikes in AT-Pyri/TiO_2 electrodes. These spikes are much more intense than in blank TiO_2, and they increase as the applied potential decreases, in agreement with previous reports [42]. The decline in the peak current density during the on position is particularly pronounced in the initial irradiation pulse and at the beginning of each pulse. After that, the decrease in j_{ph} continues steadily within each pulse and during the whole 5 min experiment. In the above mentioned reference, the pulse shape was simulated by a double exponential decay, and it was associated with at least two capacitive processes involving local electron trapping and de-trapping [42]. More specifically, the spikes might arise from electron recombination with photooxidation intermediates [43], which would be associated with the above-mentioned AT-Pyri redox couple in the CV range of −0.1 to −0.5 V (Fig. 2.b). Therefore, the presence of spikes is linked to a lack of stability. In fact, the dye is severely degraded after five minutes under those operation conditions, losing its starting orange color.

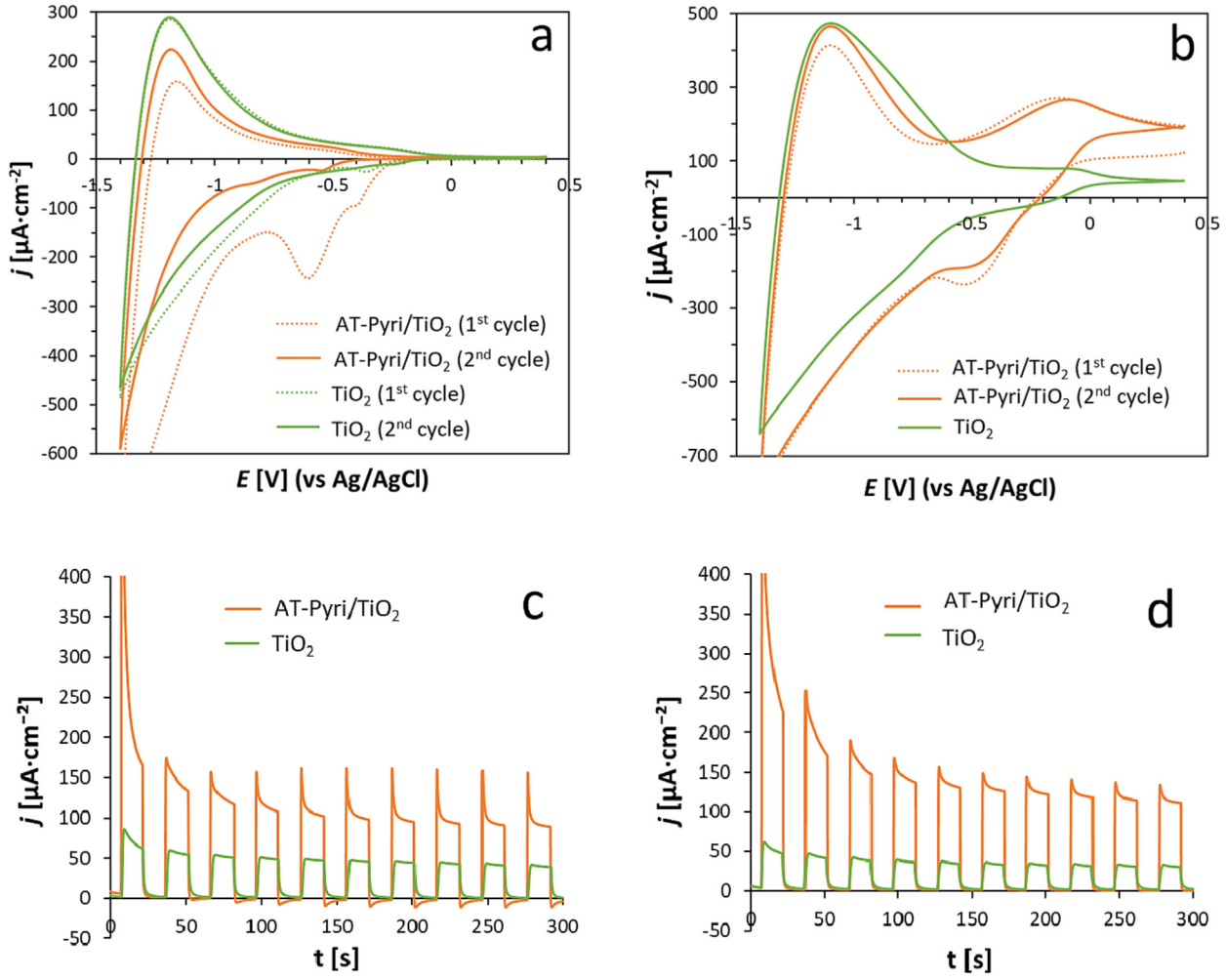

Fig. 2. Electrochemical and photoelectrochemical studies in 0.1 M Na_2SO_4: a) CV scans in the dark, starting at 0.4 V vs Ag/AgCl; b) CV scans under AM1.5G light irradiation; c) on–off transient photocurrent measurements at $E = -0.1$ V; and d) transient photocurrent at $E = 0$ V vs Ag/AgCl.

Fig. 3 shows the effect of sacrificial agents on the photoelectrochemical response of the AT-Pyri/TiO_2 electrode. In CV scans under irradiation (Fig. 3.a), the onset potential at which a photocurrent is observed is maintained in the presence of MeOH, but it clearly decreases from −0.6 to −0.8 V when TEOA is used. This fact points out that the presence of TEOA facilitates charge transfer. Transient photocurrent experiments (Fig. 3.b) also reveal changes with respect to measurements in the Na_2SO_4 electrolyte without any sacrificial agent (Fig. 2.d): current spikes decrease, and even totally disappear upon the addition of TEOA. Moreover, the "on-part" of the transient profile in TEOA keeps rising in the measurement time scale. Although MeOH and particularly ethylenediaminetetraacetate (EDTA) produce high j_{ph} values, the decrease at the end of the 5 min measurement and the color change indicates the degradation of AT-Pyri, just as in the case when no sacrificial agent is added. In contrast, the j_{ph} value in TEOA remains stable after the 5 min experiment.

The addition of certain sacrificial agents such as hydroquinone (H_2Q), potassium iodide (KI), and diethylenediamine (DEDA) may increase the current at the beginning of the 5 min experiment, but it decays afterwards. Other reactants, including MeOH, EDTA, and TEOA result in an increase in the j_{ph} value even after 5 min of experiment (Fig. 3.c). However, the real stability of AT-Pyri is only achieved in TEOA and a minimum concentration of 0.01 M TEOA is required to stabilize the dye (Fig. 3.d). Additionally, we observed that TEOA retains its stabilizing effect even in the presence of another sacrificial agent such as MeOH. Importantly, mixtures of MeOH and TEOA lead to increased j_{ph} values with a decrease in the relative concentration of TEOA (Fig. 3.d). Even so, it is confirmed for the mixtures that the original colour of AT-Pyri is only kept if at least 0.01 M of TEOA is added to the electrolyte. While TEOA has been widely used by other research groups with dye-sensitized electrodes, its particular stabilizing effect has not been compared to other sacrificial agents [22,23,44,45].

Most of the photocurrent values that are reported in the literature for D-π-A dye/TiO_2 electrodes fall in the range of 100 μA·cm^{-2} [6,8,16,17,21,22,44], while a few reach 1 mA·cm^{-2} [15,19,20]. The value of photocurrent might depend on cell configuration; in any case, the improvement of AT-Pyri/TiO_2 above the commercial TiO_2 is remarkable, according to the above mentioned literature. To definitively confirm the stability of the AT-Pyri/TiO_2 electrode in the TEOA electrolyte, we performed a series of experiments applying a constant potential (0 or 0.4 V) for 5 h (Fig. 4). The AT-Pyri/TiO_2 electrode in 0.1 M Na_2SO_4 lost the initial j_{ph} level, and its characteristic orange colour as well, at both 0.4 and 0 V of working potential. In the presence of TEOA, the j_{ph} value increases with time during 2 h, and then it decays slightly (Fig. 4.b). This initial activation has to be associated with the effect of TEOA reaction products on the dye-sensitized interface. The decay after 3 h seems analogous to that occurring in the bare TiO_2 electrode (Fig. 4.b), so it might take place by blocking of photoactive sites on TiO_2. Overall, the AT-Pyri/TiO_2 electrode keeps a high j_{ph}

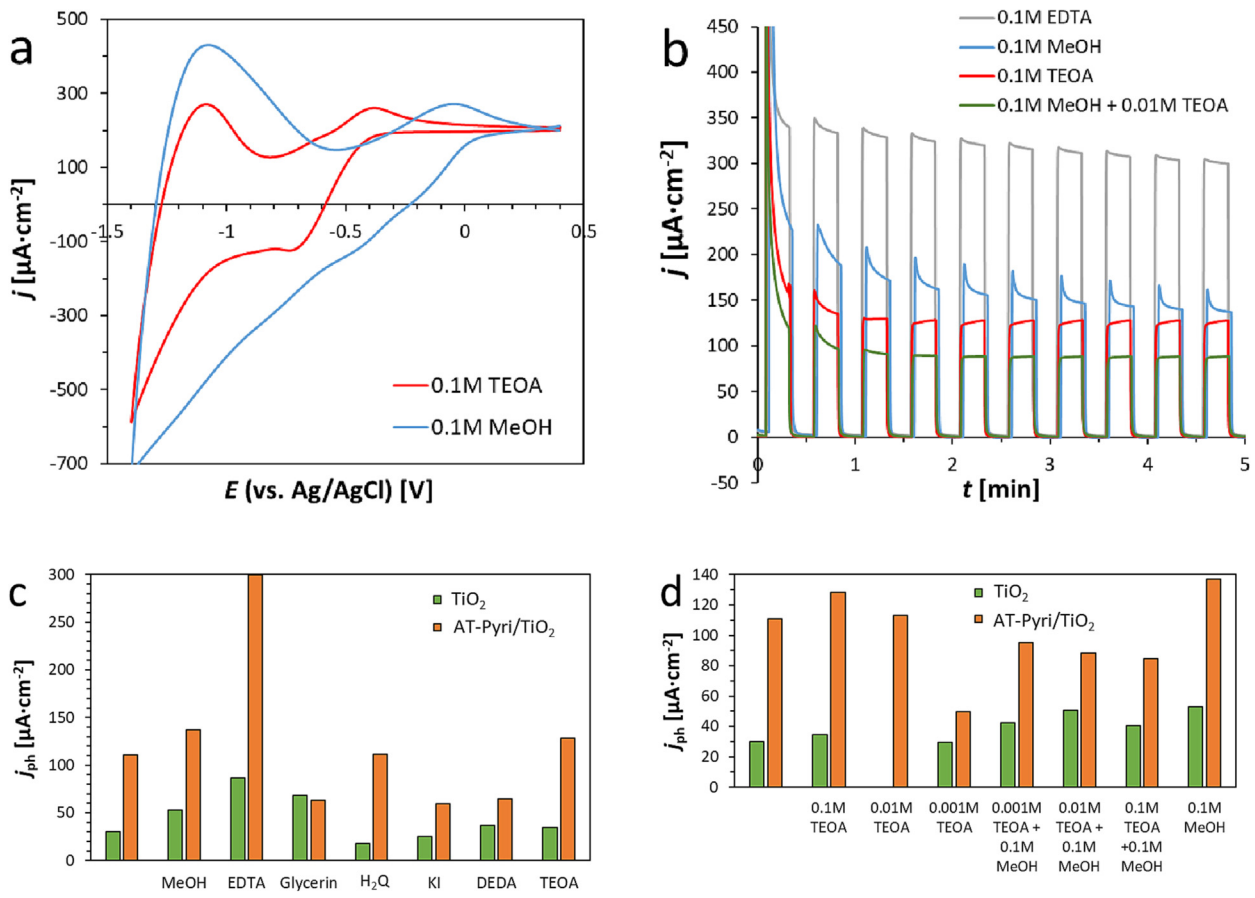

Fig. 3. Photoelectrochemical studies on AT-Pyri/TiO_2 in 0.1 M Na_2SO_4 adding different sacrificial reagents: a) CV scan starting at $E = 0.4$ V vs Ag/AgCl under continuous AM1.5G light irradiation; b) on–off transient photocurrent measurements at $E = 0$ V; c) photocurrent after 5 min, from transient photocurrent measurements at $E = 0$ V, adding a 0.1 M concentration of different sacrificial reagents; and d) photocurrent after 5 min in different mixtures of MeOH and TEOA.

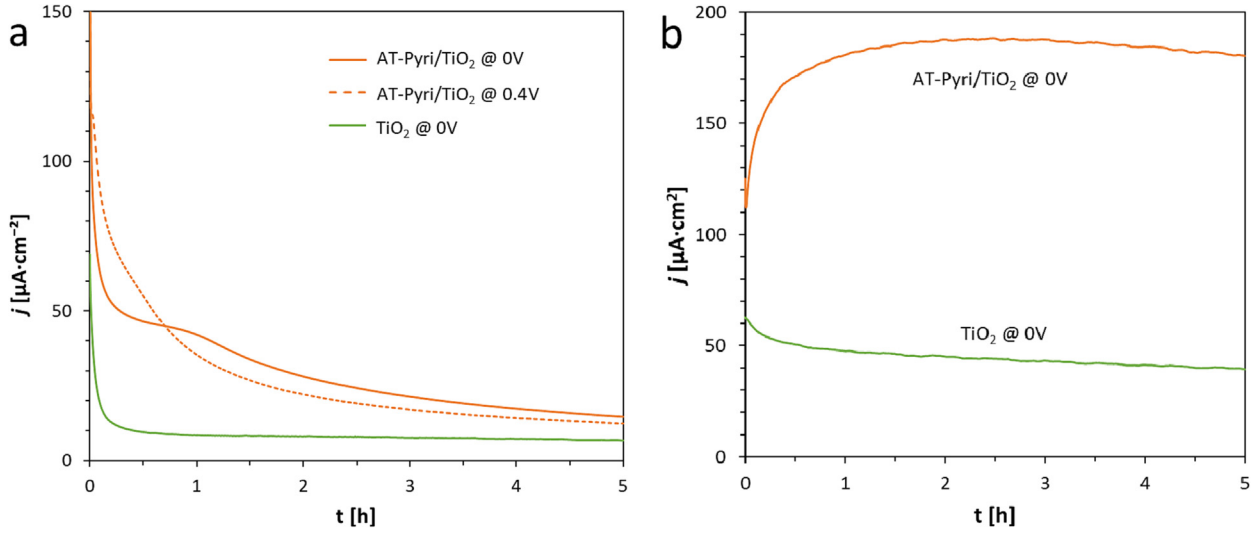

Fig. 4. Stability measurements at a constant potential E (either 0.4 or 0 V vs Ag/AgCl) and under A1.5G irradiation in: a) 0.1 M Na_2SO_4; and b) 0.1 M Na_2SO_4 + 0.1 M TEOA.

value after 5 h of experiment in TEOA, without any visual evidence of degradation.

Finally, we performed additional experiments intending to clarify the working mechanism of the AT-Pyri/TiO_2 electrode. Measurements with the monochromator (Fig. 5) prove that AT-Pyri has an impressive sensitizing effect on the electrode, yielding a photocurrent in most of the visible region. The action spectra (Fig. 5) can be intuitively related to the absorption spectrum of AT-Pyri (Fig. 1.b). Therefore, electrons from the AT-Pyri HOMO are excited to the LUMO level by light irradiation and then transferred to the FTO collector through the TiO_2 layer

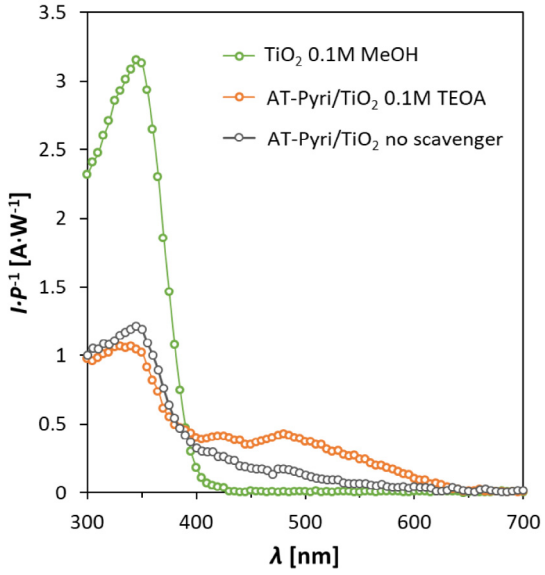

Fig. 5. Action spectra at a constant potential of 0 V vs Ag/AgCl in 0.1 M Na_2SO_4 as the base electrolyte.

(Fig. 6). Since the AT-Pyri HOMO level is higher in energy than the O_2/H_2O reduction potential, the AT-Pyri molecule cannot recover its electron from water, and eventually suffers degradation.

Sacrificial agents typically have redox potentials above that of O_2/H_2O. The potential for CO_2 reduction to MeOH (E CO_2/CH_3OH) has been located as high as 0.02 V vs the standard hydrogen electrode (SHE), close to the potential of H^+ reduction to H_2. However, the process kinetics of MeOH oxidation is complex due to the formation of surface intermediates, resulting in high overpotentials [46,47]. This fact might explain the inability of MeOH to preserve AT-Pyri from oxidative degradation. The potential for the reduction of $TEOA^+$ has been located in the range of 0.82–0.84 V vs SHE [22,23], which agrees with the preservation of AT-Pyri in our experiments. More significantly, this fact indicates a highly efficient electron transfer from TEOA to AT-Pyri$^+$ to keep the chemical integrity of the dye molecule.

4. Conclusions

A new metal-free D-π-A dye (AT-Pyri) was synthesized and adsorbed on nanoparticle TiO_2/FTO electrodes for their application in water splitting. The AT-Pyri/TiO_2 photoanode shows increased photocurrent compared to the TiO_2 blank in the Na_2SO_4 electrolyte at neutral pH. Transient photocurrent measurements on AT-Pyri/TiO_2 show spikes and a progressive decrease in photocurrent. Spikes depend on voltage and the presence of sacrificial agents. Among various tested sacrificial agents (MeOH, glycerin, EDTA, hydroquinone, KI), the AT-Pyri/TiO_2 electrode is completely stabilized only in the presence of a certain concentration of TEOA (minimum 0.01 M). The TEOA provides higher stability to the AT-Pyri dye in the presence of other additives such as MeOH. The stabilization in TEOA solutions is associated with the elimination of transient photocurrent spikes, together with the persistence of both the photocurrent level and the electrode orange colour after the 5 h chronoamperometry experiments. Finally, the photocurrent action spectrum clearly demonstrates the sensitization effect of AT-Pyri on TiO_2. The AT-Pyri dye as a photosensitizer in the TiO_2 photoanode provides a remarkable and maintained photocurrent in the presence of TEOA, encouraging further research in highly efficient stable dye-sensitized photoelectrodes for the application to water splitting.

CRediT authorship contribution statement

A. Ansón-Casaos: Conceptualization, Data curation, Writing – original draft. **C. Martínez-Barón:** Methodology, Validation, Investigation. **S. Angoy-Benabarre:** Investigation. **J. Hernández-Ferrer:** Methodology. **A.M. Benito:** Writing – review & editing, Funding acquisition. **W.K. Maser:** Writing – review & editing, Funding acquisition. **M.J. Blesa:** Methodology, Writing – review & editing, Supervision.

Declaration of Competing Interest

The authors declare that they have no known competing financial interests or personal relationships that could have appeared to influence the work reported in this paper.

Acknowledgements

Special thanks are directed to Dr. B. Villacampa for profilometer measurements, and to the ICB analysis services. Financial support from Spanish MICINN/AEI under projects PID2019-104272RB-C51/AEI/10.13039/501100011033 and PID2019-104307GB-100/AEI/10.13039/501100011033, and the Diputación General de Aragón-European Social Found under projects T03-20R and E47-20R is acknowledged.

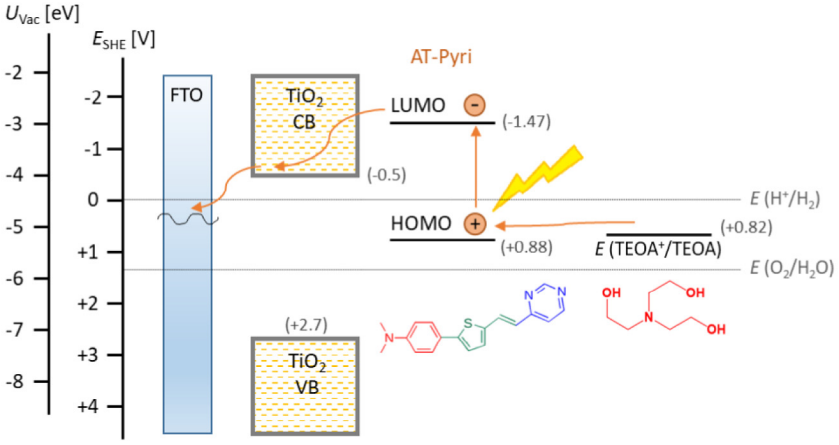

Fig. 6. Proposed mechanism of the sensitization of TiO_2 by AT-Pyri, and its durability in the presence of TEOA. Numeric potentials referred to the SHE. Energy levels for AT-Pyri extracted from [34].

References

[1] M. Ni, M.K.H. Leung, D.Y.C. Leung, K. Sumathy, A review and recent developments in photocatalytic water-splitting using TiO_2 for hydrogen production, Renew. Sust. Ener. Rev. 11 (2007) 401–425, https://doi.org/10.1016/j.rser.2005.01.009.

[2] X. Zhang, T. Peng, S. Song, Recent advances in dye-sensitized semiconductor systems for photocatalytic hydrogen production, J. Mater. Chem. A 4 (2016) 2365–2402, https://doi.org/10.1039/c5ta08939e.

[3] B. Cecconi, N. Manfredi, T. Montini, P. Fornasiero, A. Abbotto, Dye-sensitized solar hydrogen production: the emerging role of metal-free organic sensitizers, Eur. J. Org. Chem. (2016) 5194–5215, https://doi.org/10.1002/ejoc.201600653.

[4] A. Ansón-Casaos, J. Hernández-Ferrer, L. Vallan, H. Xie, M. Lira-Cantú, A.M. Benito, W.K. Maser, Functionalized carbon dots on TiO_2 for perovskite photovoltaics and stable photoanodes for water splitting, Int. J. Hydrogen Energy 46 (2021) 12180–12191, https://doi.org/10.1016/j.ijhydene.2020.03.077.

[5] J.T. Kirner, R.G. Finke, Water-oxidation photoanodes using organic light-harvesting materials: a review, J. Mater. Chem. A 5 (2017) 19560–19592, https://doi.org/10.1039/c7ta05709a.

[6] M.N. Collomb, D.V. Morales, C.N. Astudillo, B. Dautreppe, J. Fortage, Hybrid photoanodes for water oxidation combining a molecular photosensitizer with a metal oxide oxygen-evolving catalyst, Sust. Ener. Fuels 4 (2020) 31–49, https://doi.org/10.1039/c9se00597h.

[7] N. Queyriaux, N. Kaeffer, A. Morozan, M. Chavarot-Kerlidou, V. Artero, Molecular cathode and photocathode materials for hydrogen evolution in photoelectrochemical devices, J. Photochem. Photobiol. C: Photochem. Rev. 25 (2015) 90–105, https://doi.org/10.1016/j.photochemrev.2015.08.001.

[8] C. Decavoli, C.L. Boldrini, N. Manfredi, A. Abbotto, Molecular organic sensitizers for photoelectrochemical water splitting, Eur. J. Inorg. Chem. (2020) 978–999, https://doi.org/10.1002/ejic.202000026.

[9] J.F. Huang, Y. Lei, T. Luo, J.M. Liu, Photocatalytic H_2 production from water by metal-free dye-sensitized TiO_2 semiconductors: the role and development process of organic sensitizers, ChemSusChem 13 (2020) 5863–5895, https://doi.org/10.1002/cssc202001646.

[10] B. Liu, W. Zhu, Q. Zhang, W. Wu, M. Xu, Z. Ning, Y. Xie, H. Tian, Conveniently synthesized isophorone dyes for high efficiency dye-sensitized solar cells: tuning photovoltaic performance by structural modification of donor group in donor–p–acceptor system, Chem. Commun. (2009) 1766–1768, https://doi.org/10.1039/b820964b.

[11] I. Duerto, E. Colom, J.M. Andres-Castan, S. Franco, J. Garín, J. Orduna, B. Villacampa, M.J. Blesa, DSSCs based on aniline derivatives functionalized with a tert-butyldimethylsilyl group and the effect of the π-spacer, Dyes Pigm. 148 (2018) 61–71, https://doi.org/10.1016/j.dyepig.2017.07.063.

[12] R. Abe, K. Shinmei, K. Hara, B. Ohtani, Robust dye-sensitized overall water splitting system with two-step photoexcitation of coumarin dyes and metal oxide semiconductors, Chem. Commun. (2009) 3577–3579, https://doi.org/10.1039/b905935k.

[13] A. Hagfeldt, G. Boschloo, L. Sun, L. Kloo, H. Pettersson, Dye-sensitized solar cells, Chem. Rev. 110 (2010) 6595–6663, https://doi.org/10.1021/cr900356p.

[14] Y. Ooyama, K. Uenaka, J. Ohshita, Development of a functionally separated D–π-A fluorescent dye with a pyrazyl group as an electron-accepting group for dye-sensitized solar cells, Org. Chem. Front. 2 (2015) 552–559, https://doi.org/10.1039/C5QO00050E.

[15] K.R. Wee, B.D. Sherman, M.K. Brennaman, M.V. Sheridan, A. Nayak, L. Alibabaei, T.J. Meyer, An aqueous, organic dye derivatized SnO_2/TiO_2 core/shell photoanode, J. Mater. Chem. A 4 (2016) 2969–2975, https://doi.org/10.1039/c5ta06678f.

[16] L. Alibabaei, R.J. Dillon, C.E. Reilly, M.K. Brennaman, K.R. Wee, S.L. Marquard, J. M. Papanikolas, T.J. Meyer, Chromophore-catalyst assembly for water oxidation prepared by atomic layer deposition, ACS Appl. Mater. Interfaces 9 (2017) 39018–39026, https://doi.org/10.1021/acsami.7b11905.

[17] M.S. Eberhart, D. Wang, R.N. Sampaio, S.L. Marquard, B. Shan, M.K. Brennaman, G.J. Meyer, C. Dares, T.J. Meyer, Water photo-oxidation initiated by surface-bound organic chromophores, J. Am. Chem. Soc. 139 (2017) 16248–16255, https://doi.org/10.1021/jacs.7b08317.

[18] T.G.U. Ghobadi, M. Buyuktemiz, E.A. Yildiz, D.B. Yildiz, H.G. Yaglioglu, Y. Dede, E. Ozbay, F. Karadas, A robust, precious-metal-free dye-sensitized photoanode for water oxidation: a nanosecond-long excited-state lifetime through a Prussian blue analog, Angew. Chem. Int. Ed. 59 (2020) 4082–4090, https://doi.org/10.1002/anie.201914743.

[19] H. Ding, M. Xu, S. Zhang, F. Yu, K. Kong, Z. Shen, J. Hua, Organic blue-colored D-A-π-A dye-sensitized TiO_2 for efficient and stable photocatalytic hydrogen evolution under visible/near-infrared-light irradiation, Renew. Energy 155 (2020) 1051–1059, https://doi.org/10.1016/j.renene.2020.04.009.

[20] O. Suryani, Y. Higashino, H. Sato, Y. Kubo, Visible-to-near-infrared light-driven photocatalytic hydrogen production using dibenzo-BODIPY and phenothiazine conjugate as organic photosensitizer, ACS Appl. Energy Mater. 2 (2019) 448–458, https://doi.org/10.1021/acsaem.8b01474.

[21] B. Yildiz, E. Güzel, D. Akyüz, B.S. Arslan, A. Koca, M.K. Sener, Unsymmetrically pyrazole-3-carboxylic acid substituted phthalocyanine-based photoanodes for use in water splitting photoelectrochemical and dye-sensitized solar cells, Solar Energy 191 (2019) 654–662, https://doi.org/10.1016/j.solener.2019.09.043.

[22] E. Aslan, M. Karaman, G. Yanalak, H. Bilgili, M. Can, F. Ozel, Synthesis of novel tetrazine based D-π-A organic dyes for photoelectrochemical and photocatalytic hydrogen evolution, J. Photochem. Photobiol. A: Chem. 390 (2020), https://doi.org/10.1016/j.jphotochem.2019.112301 112301.

[23] Y. Zhong, Y. Lei, J. Huang, L. Xiao, X. Chen, T. Luo, S. Qin, J. Guo, J. Liu, Design of alkaline pyridil acceptor-based calix [4]arene dye and synthesis of stable calixarene-TiO_2 porous hybrid materials for efficient photocatalysis, J. Mater. Chem. A 8 (2020) 8883–8891, https://doi.org/10.1039/D0TA00754D.

[24] Y. Pellegrin, F. Odobel, Sacrificial electron donor reagents for solar fuel production, Comptes Rendus Chimie 20 (2017) 283–295, https://doi.org/10.1016/j.crci.2015.11.026.

[25] J. Hernández-Ferrer, A. Ansón-Casaos, S. Víctor-Román, O. Sanahuja-Parejo, M.T. Martínez, B. Villacampa, A.M. Benito, W.K. Maser, Photoactivity improvement of TiO_2 electrodes by thin hole transport layers of reduced graphene oxide, Electrochimica Acta 298 (2019) 279–287, https://doi.org/10.1016/j.electacta.2018.12.085.

[26] G.K. Mor, O.K. Varghese, R.H.T. Wilke, S. Sharma, K. Shankar, T.J. Latempa, K. Choi, C.A. Grimes, p-type Cu-Ti-O nanotube arrays and their use in self-biased heterojunction photoelectrochemical diodes for hydrogen generation, Nano Lett. 8 (2008) 1906–1911, https://doi.org/10.1021/nl080572y.

[27] G.B. Saupe, T.E. Mallouk, W. Kim, R.H. Schmehl, Visible light photolysis of hydrogen iodide using sensitized layered metal oxide semiconductors: the role of surface chemical modifications in controlling back electron transfer reactions, J. Phys. Chem. B 101 (1997) 2508–2513, https://doi.org/10.1021/jp9625319.

[28] R. Abe, K. Sayama, H. Arakawa, Efficient hydrogen evolution from aqueous mixture of I and acetonitrile using merocyanine dye-sensitized Pt/TiO_2 photocatalyst under visible light irradiation, Chem. Phys. Lett. 362 (2002) 441–444, https://doi.org/10.1016/S0009-2614(02)01140-5.

[29] K. Kalyanasundaram, J. Kiwi, M. Grätzel, Hydrogen evolution from water by visible light, a homogeneous three component test system for redox catalysis, Helvetica Chimica Acta 61 (1978) 2720–2730, https://doi.org/10.1002/hlca.19780610740.

[30] R. Abe, K. Hara, K. Sayama, K. Domen, H. Arakawa, Steady hydrogen evolution from water on Eosin Y-fixed TiO_2 photocatalyst using a silane-coupling reagent under visible light irradiation, J. Photochem. Photobiol. A Chem. 137 (2000) 63–69, https://doi.org/10.1016/S1010-6030(00)00351-8.

[31] Y. Li, M. Guo, S. Peng, G. Lu, S. Li, Formation of multilayer-Eosin Y-sensitized TiO_2 via Fe^{3+} coupling for efficient visible-light photocatalytic hydrogen evolution, Int. J. Hydrogen Energy 34 (2009) 5629–5636, https://doi.org/10.1016/j.ijhydene.2009.05.100.

[32] J. Lee, J. Kwak, K.C. Ko, J.H. Park, J.H. Ko, N. Park, E. Kim, D.H. Ryu, T.K. Ahn, J. Y. Lee, S.U. Son, Phenothiazine-based organic dyes with two anchoring groups on TiO_2 for highly efficient visible light-induced water splitting, Chem. Commun. 48 (2012) 11431–11433, https://doi.org/10.1039/c2cc36501d.

[33] W. Jones, D.J. Martin, A. Caravaca, A.M. Beale, M. Bowker, T. Maschmeyer, G. Hartley, A. Masters, A comparison of photocatalytic reforming reactions of methanol and triethanolamine with Pd supported on titania and graphitic carbon nitride, Appl. Catal. B Environ. 240 (2019) 373–379, https://doi.org/10.1016/j.apcatb.2017.01.042.

[34] I. Duerto, S. Sarasa, D. Barrios, J. Orduna, B. Villacampa, M.J. Blesa, Enhancing the temporal stability of DSSCs with novel vinylpyrimidine anchoring and accepting group, Dyes Pigm. 203 (2022), https://doi.org/10.1016/j.dyepig.2022.110310 110310.

[35] F. Quist, C.M.L. Vande Velde, D. Didier, A. Teshome, I. Asselberghs, K. Clays, S. Sergeyev, Push–pull chromophores comprising benzothiazolium acceptor and thiophene auxiliary donor moieties: synthesis, structure, linear and quadratic non-linear optical properties, Dyes Pigm. 81 (2009) 203–210, https://doi.org/10.1016/j.dyepig.2008.10.004.

[36] M.I. Zaki, M.A. Hasan, F.A. Al-Sagheer, L. Pasupulety, In situ FTIR spectra of pyridine adsorbed on SiO_2-Al_2O_3, TiO_2, ZrO_2 and CeO_2: general considerations for the identification of acid sites on surfaces of finely divided metal oxides, Colloids Surf. A 190 (2001) 261–274, https://doi.org/10.1016/S0927-7757(01)00690-2.

[37] V. Vishwanathan, H.S. Roh, J.W. Kim, K.W. Jun, Surface properties and catalytic activity of TiO_2–ZrO_2 mixed oxides in dehydration of methanol to dimethyl ether, Catal. Lett. 96 (2004) 23–28, https://doi.org/10.1023/B:CATL.0000029524.94392.9f.

[38] M.M. Mohamed, W.A. Bayoumy, M. Khairy, M.A. Mousa, Synthesis of micro–mesoporous TiO_2 materials assembled via cationic surfactants: Morphology, thermal stability and surface acidity characteristics, Microporous Mesoporous Mater. 103 (2007) 174–183, https://doi.org/10.1016/j.micromeso.2007.01.052.

[39] Y. Ooyama, T. Nagano, S. Inoue, I. Imae, K. Komaguchi, J. Ohshita, Y. Harima, Dye-sensitized solar cells based on donor-π-acceptor fluorescent dyes with a pyridine ring as an electron-withdrawing-injecting anchoring group, Chem. Eur. J. 17 (2011) 14837–14843, https://doi.org/10.1002/chem.201101923.

[40] A. Turkovic, M. Ivanda, A. Drasner, V. Vranesa, M. Persin, Raman spectroscopy of thermally annealed TiO_2 thin films, Thin Solid Films 198 (1991) 199–205, https://doi.org/10.1016/0040-6090(91)90338-X.

[41] A.B. Marco, P. Mayorga Burrezo, L. Mosteo, S. Franco, J. Garín, J. Orduna, B.E. Diosdado, B. Villacampa, J.T. López Navarrete, J. Casado, R. Andreu, Polarization, second-order nonlinear optical properties and electrochromism in 4H-pyranylidene chromophores with a quinoid/aromatic thiophene ring bridge, RSC Adv. 5 (2015) 231–242, https://doi.org/10.1039/C4RA12791A.

[42] N.G. Ghosh, A. Sarkar, S.S. Zade, The type-II n-n inorganic/organic nano-heterojunction of Ti^{3+} self-doped TiO_2 nanorods and conjugated co-polymers for photoelectrochemical water splitting and photocatalytic dye degradation, Chem. Engin. J. 407 (2021), https://doi.org/10.1016/j.cej.2020.127227 127227.

[43] T. Berger, D. Monllor-Satoca, M. Jankulovska, T. Lana-Villarreal, R. Gómez, The electrochemistry of nanostructured titanium dioxide electrodes, ChemPhysChem. 13 (2012) 2824–2875, https://doi.org/10.1002/cphc.201200073.
[44] L. Sang, L. Lei, J. Lin, H. Ge, Co-sensitization of TiO_2 electrode with Eosin Y dye and carbon dots for phototelectrochemical water splitting: The enhanced dye adsorption and the charge transfer route, Int. J. Hydrogen Ener. 42 (2017) 29686–29693, https://doi.org/10.1016/j.ijhydene.2017.10.034.
[45] L. Sang, S. Zhang, J. Zhang, Z. Yu, G. Bai, C. Du, TiO_2 nanotube arrays decorated with plasmonic Cu, CuO nanoparticles, and eosin Y dye as efficient photoanode for water splitting, Mater. Chem. Phys. 231 (2019) 27–32, https://doi.org/10.1016/j.matchemphys.2019.04.018.
[46] T. Iwasita, Electrocatalysis of methanol oxidation, Electrochim. Acta 47 (2002) 3663–3674, https://doi.org/10.1016/S0013-4686(02)00336-5.
[47] H. Okamoto, T. Gojuki, N. Okano, T. Kuge, M. Morita, A. Maruyama, Y. Mukouyama, Oxidation of formic acid and methanol and their potential oscillations under no or little water conditions, Electrochim. Acta 136 (2014) 385–395, https://doi.org/10.1016/j.electacta.2014.05.135.